Enhanced Nonlinear Double Excitation of He in Intense Extreme Ultraviolet Laser Fields

A. Hishikawa,[1,2,3,*] M. Fushitani,[1,3] Y. Hikosaka,[3,4] A. Matsuda,[1,2,3] C.-N. Liu,[5] T. Morishita,[6,7,†] E. Shigemasa,[2,3] M. Nagasono,[3] K. Tono,[8] T. Togashi,[8] H. Ohashi,[3,8] H. Kimura,[3,8] Y. Senba,[8] M. Yabashi,[3,8] and T. Ishikawa[3]

[1]*Department of Chemistry, Graduate School of Science, Nagoya University, Nagoya, Aichi 464-8602, Japan*
[2]*Institute for Molecular Science, National Institutes of Natural Sciences, Okazaki, Aichi 444-8585, Japan*
[3]*RIKEN/SPring-8, Sayo, Hyogo 679-5148, Japan*
[4]*Department of Environmental Science, Niigata University, Niigata, Niigata 950-2181, Japan*
[5]*Department of Physics, Fu-Jen Catholic University, Taipei 24205, Taiwan*
[6]*Department of Engineering Science, University of Electro-Communications, Chofu, Tokyo 182-8585, Japan*
[7]*PRESTO, Japan Science and Technology Agency, Kawaguchi, Saitama 332-0012, Japan*
[8]*JASRI/SPring-8, Sayo, Hyogo 679-5198, Japan*

(Received 23 July 2011; published 6 December 2011)

Nonlinear, three-photon double excitation of He in intense extreme ultraviolet free-electron laser fields (~ 24.1 eV, ~ 5 TW/cm^2) is presented. Resonances to the doubly excited states converging to the He^+ $N = 3$ level are revealed by the shot-by-shot photoelectron spectroscopy and identified by theoretical calculations based on the time-dependent Schrödinger equation for the two-electron atom under a laser field. It is shown that the three-photon double excitation is enhanced by intermediate Rydberg states below the first ionization threshold, giving a greater contribution to the photoionization yields than the two-photon process by more than 1 order of magnitude.

DOI: 10.1103/PhysRevLett.107.243003 PACS numbers: 32.80.Rm, 32.80.Fb, 32.80.Zb

Multiphoton ionization is a typical nonlinear response of atoms and molecules exposed to intense laser fields [1–3]. In contrast to the infrared or visible regime where the valence electrons are of primary importance for the response, a number of different pathways are open in extreme ultraviolet (EUV) or x-ray laser fields, because electrons can participate in the ionization from both the valence and the inner-shell levels due to the high photon energy. Modeling of nonlinear processes in such a high frequency laser field is important in a broad range of pure and applied research, including single-shot x-ray imaging [4], ultrafast optics [5], and fusion and astrophysics [6], and requires a detailed understanding of the underlying physics controlling the multiphoton processes.

Isolated atoms have been subjected to a number of experimental studies as a benchmark to clarify the possible pathways leading to the ejection of electrons [7–16]. With only a few exceptions [11], the pathways observed so far have been well understood by a single active electron picture in which the laser pulse primarily drives a single electron in each ionization step either from a valence or inner-shell level. Here we present a new nonlinear photoabsorption pathway in EUV involving a joint excitation of two electrons (Fig. 1), which provides a substantial enhancement of the multiphoton absorption to dominate the photoionization process at large laser field intensities (~ 5 TW/cm^2).

The experiment was performed using the SCSS Test Accelerator [17] at SPring-8, which delivered linearly polarized ultrashort (~ 100 fs [17]) intense (~ 10 μJ/pulse) EUV free-electron laser (FEL) pulses at a 20 Hz repetition rate. The FEL pulses were focused with a pair of elliptical and cylindrical mirrors into about 25 μm (FWHM) in diameter with a total throughput of 35%, which provided the laser field intensity of ~ 5 TW/cm^2 at the focal spot. The averaged intensities of the second and third harmonics are 0.1% and 1% of that of the fundamental FEL, respectively. The nonlinear response of He was studied by photoelectron spectroscopy using a 1.5-m-long magnetic-bottle-type electron spectrometer with a 4π-sr detection angle. The kinetic energies

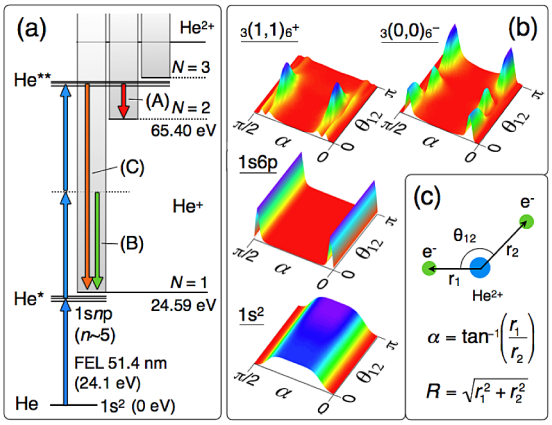

FIG. 1 (color online). (a) Scheme of three-photon double excitation of He using EUV FEL. (b) Density plots of two-electron wave functions in hyperspherical coordinates [31,32] for the $1s^2$ ground state, the $1s6p$ Rydberg state, and the $^1P^o$ doubly excited states, $_3(1,1)_6{}^+$ and $_3(0,0)_6{}^-$. Strong angular correlation is seen in the doubly excited states. (c) Definition of the hyperspherical coordinates, α and R, and the angle θ_{12}.

of the photoelectrons were calibrated by measuring Xe $4d$ Auger lines [18,19] from single-photon ionization with a third harmonics ($\sim$ 72 eV) of FEL. The energy resolution was $\sim$5% for electrons below 20 eV. An electrostatic retarder was used for high-resolution measurements. The comparison with an intensity calibrated reference of the Xe $4d$ Auger spectrum [19] shows that the detection efficiency is almost constant in the range investigated in the present study.

The spectrum of the current FELs operated in the self-amplified spontaneous emission mode has a large shot-by-shot fluctuation both in wavelength and intensity [17,20,21]. As demonstrated recently [14], the high collection efficiency of the magnetic-bottle photoelectron spectrometer allows a simultaneous recording of the FEL spectrum and the nonlinear photoelectron spectrum in a single shot. The single-shot photoelectron spectroscopy provides a unique means to uncover the mechanism of the multiphoton absorption, particularly the resonance effect, which can be blurred by averaging over many FEL shots [14].

Figure 2(a) shows a photoelectron spectrum of He at a FEL wavelength of 51.4 nm (corresponding to a photon energy of 24.1 eV), averaged over 15 000 FEL shots. A small amount of Xe was introduced in the chamber for the single-shot monitoring of the FEL spectrum [14], which appeared as the doublet peaks at 10.8 and 12.2 eV due to the Xe^+ $5p^{-1}$ spin-orbit components by single-photon ionization. In addition, three peaks (A), (B), and (C) are identified in the spectra at 6.9, 24, and 48 eV, respectively. The observed energies allow us to assign peak (B) to electrons emitted from the two-photon energy level (48.2 eV) to the He^+ $N = 1$ state, and the peaks (A) and (C) to those from the three-photon level (72.3 eV) to the He^+ $N = 2$ and $N = 1$ states, respectively [see Fig. 1(a)].

The details of the photoionization process can be understood from the FEL intensity dependence. When the fundamental FEL intensity is reduced by a gas attenuator, a significant suppression of the peak (A) is observed [Fig. 2(a)]. The shot-by-shot analysis of the peak intensity in Fig. 2(b) shows a steep slope, $k = 2.3(1)$, indicating that the photoelectron peak (A) originates dominantly from a nonlinear photoabsorption process. On the other hand, only moderate dependences are observed for peaks (B) and (C). The constant backgrounds of peaks (B) and (C), appearing as the asymptotic values at low FEL intensities in Fig. 2(b), are attributed to the second and third order harmonics, which are only slightly attenuated by the Ar gas attenuator (3% and 5%, respectively [22]) in the range investigated in the present study. No clear correlation between the harmonics and the fundamental FEL was identified within the present statistical uncertainty. It should be noted that the contribution from the third harmonics appears more significantly in peak (C) than in peak (A), because the one-photon absorption in this energy region ($\sim$ 72 eV) leads

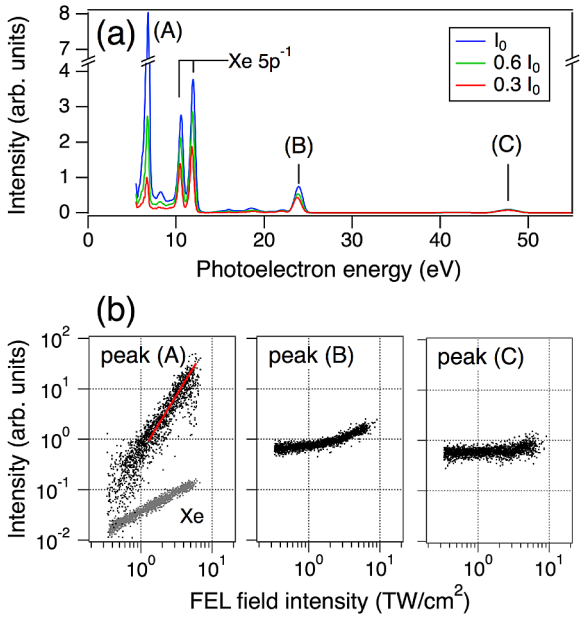

FIG. 2 (color online). (a) Averaged photoelectron spectrum of He in intense EUV laser fields (24.1 eV). A retardation voltage of -5.5 eV is applied to obtain a high spectral resolution. The doublet peaks around 11 eV are due to Xe introduced for the shot-by-shot photoelectron spectroscopy, while the three peaks (A), (B), and (C) are from He. The spectra recorded at three different fundamental FEL field intensities, $I = I_0$, $\sim 0.6 I_0$, and $\sim 0.3 I_0$, are shown in the full energy region (> 5.5 eV), where I_0 (~ 5 TW/cm^2) represents the average laser field intensity obtained with no attenuation. Because of the small peak intensity, the variation of peak (C) is hardly visible in this scale. (b) Intensities of the three He peaks plotted against the fundamental FEL field intensity. The FEL pulse intensity was monitored for each laser pulse by a photoion yield detector. In order to cover the wide range of intensity, an Ar gas attenuator placed upstream of the FEL beam line was used, which virtually affects the fundamental FEL only. The intensity of the Xe peaks is plotted against the fundamental FEL intensity for comparison. The observed slope is slightly less than 1 due to the saturation of the ionization process [14].

dominantly to the direct ionization to the $N = 1$ channel ($> 90\%$) [23,24]. The net contribution from the multiphoton absorption of the fundamental FEL can be obtained by the subtraction of these backgrounds. The relative integrated peak intensities of 24:1:0.3 thus obtained for (A), (B). and (C) show that the total yields for the three-photon absorption (A) + (C) is more than 1 order larger than that for the two-photon process (B) at a field intensity of 5 TW/cm^2 [see Fig. 2(a)].

The mechanism of the enhancement of the three-photon process becomes clear by close inspection of the photoelectron spectrum. An expanded view of peak (A) plotted in Fig. 3(a) shows several subpeaks due to resonances. An insight into the origin of the fine structure is obtained by the single-shot photoelectron spectroscopy [14]. The spectral analysis based on the single-shot measurements allows

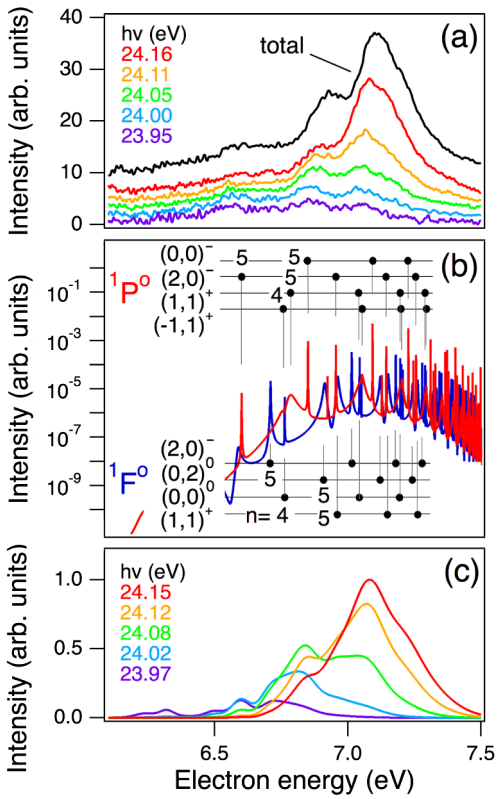

FIG. 3 (color online). Shot-by-shot photoelectron spectra and the comparison with theoretical calculations. (a) Photoelectron spectra of peak (A) for the three-photon excitation of He obtained by the shot-by-shot analysis. Different colors correspond to different mean photon energies. The total spectrum is shown on the top (solid line). (b) Theoretical three-photon photoelectron spectra (8.3 fs, 3.5 TW/cm^2) of the $^1P^o$ [light gray (red) line] and $^1F^o$ [dark gray (blue) line] doubly excited states of He decaying into $He^+(2s, 2p) + e^-$ channels at 24.15 eV in the logarithmic scale. The assignments of the $3lnl'$ doubly excited states converging to the He^+ $N = 3$ state [26–28] are also shown using the $(K, T)^A$ notation. (c) The theoretical spectra for different photon energies convoluted with a Gaussian ($E/\Delta E = 17$).

us to obtain the FEL photon energy dependence of the photoelectron spectra by utilizing the inherent fluctuation of FEL pulses.

Figure 3(a) plots the photoelectron spectra of peak (A) obtained from a shot-by-shot analysis. Here single-shot photoelectron spectra obtained at a nominal FEL photon energy of 24.1 eV were sorted by the center photon energies determined from the Xe^+ $5p^{-1}$ peak energies [see Fig. 2(a)], and then averaged within narrow photon energy ranges that divide the whole photon energy range (23.95–24.17 eV) into 5 segments. The shot-by-shot photoelectron spectra show that the positions of the observed fine peaks do not shift by the changes of the center photon energy. This finding clearly shows that some excited states in the neutral He autoionizing manifold are in three-photon resonance from the neutral ground state.

In the three-photon energy range ($\sim$ 72.3 eV), doubly excited states converging to the He^+ $N = 3$ level have been identified previously [23,25–28]. Doubly excited states of He have been a target of intensive research as the smallest system exhibiting the effects of strong electron correlation [29–34]. Because of the interaction between the two electrons, the doubly excited states cannot be described by an independent-particle model in which each electron occupies a single atomic orbital (e.g., $2s3p$) even in the first order approximation. Detailed theoretical studies [29,30,32,33] show that the electron correlation is characterized by a set of approximate quantum numbers. Here we adopt the ${}_N(K, T)_n{}^A$ notation, where N and n denote the principal quantum numbers of the inner and outer electrons, (K, T) represent their angular correlation, respectively [31,32]. The label A shows the radial correlation of the two electrons oscillating in phase ($A = +1$) and out of phase ($A = -1$), while $A = 0$ represents states with neither of these properties.

In order to securely assign the observed resonances, we solved the time-dependent Schrödinger equation (TDSE) for the two-electron atom under a laser field. The electron correlations in both discrete and continuum states below the double ionization threshold are fully taken into account by using the time-dependent hyperspherical method [35], where the box-normalized hyperspherical eigenfunctions in $0 \le R \le R_0$ ($R_0 = 1600$ a.u.) were used as the basis set for the expansion. The propagation of the time-dependent solution was performed by the second-order split operator method. The dipole approximation in the length gauge was employed to calculate the interaction with the laser fields, i.e., $V(t) = -(\boldsymbol{r}_1 + \boldsymbol{r}_2) \cdot \boldsymbol{F}(t)$, where $\boldsymbol{r}_1$ and $\boldsymbol{r}_2$ are the position vectors of the electrons centered about the nucleus [Fig. 1(c)] and $\boldsymbol{F}(t)$ is the electric field dependent on the time t. A squared sinusoidal envelope was assumed for the laser electric field. Since the computation difficulties do not allow us to solve the TDSE for a 100 fs pulse, we set the pulse duration to 8.3 fs to reproduce the effective bandwidth of the FEL ($\sim$ 0.2 eV [17]), which determines the spectral breadth of the photoelectron spectra. The photoelectron energy spectrum was calculated by integrating the transition amplitude over the 4π solid angle at the end of the laser pulse.

Figure 3(b) plots theoretical spectra obtained for an intense EUV pulse at 24.15 eV (3.5 TW/cm^2). The spectra are dominated by resonances due to $^1P^o$ and $^1F^o$ doubly excited states, exhibiting dense manifolds of sharp and broad series with different A values converging to the He^+ $N = 3$ level. In addition, consistent with earlier studies [24,36], the theoretical results indicate that these doubly excited states predominantly autoionize into the He^+ $N = 2$ channel. The theoretical branching ratio between the $N = 2$ and $N = 1$ channels is $\sim 10^2$:1 [24], which explains the observed three-photon-yield ratio (24:0.3) between peak (A) and peak (C) in Fig. 2(a).

The theoretical photoelectron spectra were calculated at different center photon energies and convoluted with the experimental width ($E/\Delta E \sim 20$) for comparison with the experimental results, as shown in Fig. 3(c). The good agreement with the experimental results in Fig. 3(a) confirms that the doubly excited states in Fig. 3(b) are resonantly populated by the three-photon absorption of FEL radiation. It should be noted that the spectra are dominated by the $^1P^o$ state, and that the $A = +1$ and -1 series have almost the same integrated peak areas and contribute equally to the convoluted spectra. For example, in the convoluted spectra for the photon energy of 24.16 eV [see Fig. 3(c)], the peak at 7.1 eV is mostly from the $_3(0, 0)_6^-$ and $_3(1, 1)_6^+$ states, while the shoulder peak at 6.8 eV is associated with $_3(0, 0)_5^-$ and $_3(1, 1)_5^+$.

In order to gain further understanding of the mechanism of the three-photon enhancement against the two-photon process, we measured photoelectron spectra with an ultrashort UV laser pulse (250 nm, >50 fs) introduced at a time delay of 50 ps after the FEL pulse. The obtained spectrum in Fig. 4 shows several peaks at ~4.5 eV due to the signals from the He $1snp\ ^1P^o$ Rydberg states [see Fig. 1(a)]. Each state exhibits a doublet structure due to the time delay between the forward and backward photoelectrons against the detector, which became visible by the narrow bandwidth of the UV laser (< 0.03 eV). No such splitting was observed with the FEL alone. The doublet structure is modeled as a sum of two normalized Gaussian functions to estimate the integrated peak intensity by the least-squares fitting to the observed spectrum, where the widths and relative intensities as well as the peak energy difference were fixed to those estimated for $n = 4$. From the integrated peak intensities thus determined, the relative populations of the Rydberg states were estimated to be 0.10, 0.48, 0.26, 0.11, and 0.04 for $n = 4$–8, respectively, by assuming that the ionization cross section scales as n^{-3} [37] (see the inset of Fig. 4).

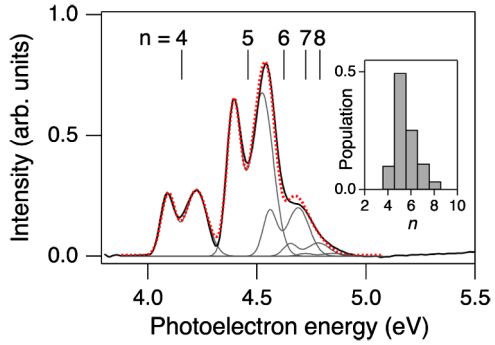

FIG. 4 (color online). UV photoelectron spectrum of He Rydberg states populated by EUV FEL. The observed spectrum (solid line) shows peaks from the $1snp$ Rydberg states by a UV pulse at 250 nm introduced at a time delay of 50 ps from the FEL pulse. The retardation voltage was −1.9 V. The doublet structure is associated with the time delay between the forward and backward photoelectron components. The relative populations of $1snp$ Rydberg states are estimated by the least-squares-fitting (dotted line) incorporating the doublet structure for each peak (gray). The relative populations are to be 0.10, 0.48, 0.26, 0.11, and 0.04 for $n = 4$–8, respectively, as shown in the inset.

The deviation of the nonlinearity for peak (A), $k = 2.3(1)$ [see Fig. 2(b)], from that expected for a nonresonant three-photon absorption ($k = 3$) supports the involvement of the intermediate resonance. The observed principal quantum number n of the Rydberg states is close to that of the outer electron in the doubly excited states [Fig. 3(b)]. This indicates that the second step of the double excitation occurs almost through the isolated core excitation observed in multicolor double excitation of alkaline earth atoms [38].

The resonance to the intermediate Rydberg states explains the enhancement of the three-photon process (A and C) against the two-photon ionization (B). Although the np Rydberg electron is only weakly bound (~ 1 eV) from the ionization threshold, the photoionization cross section in EUV is expected to be rather small due to the small overlap integral between the diffuse Rydberg state and the highly oscillatory wave function of the high-energy ionization continuum. On the contrary, the remaining $1s$ electron has a large overlap with the tightly bound $3l$ states, which enhances the nonlinear excitation to the doubly excited states at a high laser field intensity.

It is also worth noting that the three-photon $^1P^o$ spectra in Fig. 3(b) exhibit the peaks from both the $A = +1$ and -1 states, which is in marked contrast to the single-photon absorption from the ground state where only the $A = +1$ peaks appear as the major components [25]. The prominence of the $A = -1$ states in the three-photon spectra is attributed again to the resonant excitation to the intermediate Rydberg states, where no significant correlation between the $1s$ and np electrons exists due to the large interelectron distance, as depicted in the density plots of the two-electron wave function [Fig. 1(b)] expressed in the hyperspherical coordinates [Fig. 1(c)]. The lack of the electron correlation removes the propensity for the radiative transition to the $A = +1$ doubly excited states from the ground state [39,40], thus opening the pathways to the dense manifolds of all the A series of allowed symmetry ($^1P^o$ and $^1F^o$) to assist the nonlinear double excitation [15,16]. A separate theoretical calculation using the $1snp$ Rydberg state as the initial state also confirms the prominence of the $A = -1$ states as well as the preference for the nonlinear double excitation compared to the direct ionization of the Rydberg electron.

In conclusion, the present study demonstrated that the double excitation of helium occurs efficiently in intense EUV laser fields by nonlinear multiphoton absorption. The intermediate Rydberg states contribute to the enhancement of the multiphoton process by trapping the first electron driven by the laser field in the inactive states for the ionization, and by opening the pathways to all the

symmetry allowed states by the breakdown of the propensity. These mechanisms, especially the former, are universal to other systems, and should be, therefore, important in modeling the responses of more complex systems at a focus of ultrashort intense EUV and x-ray FEL pulses.

We thank C. D. Lin (Kansas State University) and J. H. D. Eland (Oxford University) for fruitful discussions and comments. We are indebted to the SCSS Test Accelerator Operation Group at RIKEN.

*hishi@chem.nagoya-u.ac.jp
†toru@pc.uec.ac.jp

[1] M. Protopapas, C. H. Keitel, and P. L. Knight, Rep. Prog. Phys. **60**, 389 (1997).
[2] J. Ullrich *et al.*, Rep. Prog. Phys. **66**, 1463 (2003).
[3] J. H. Posthumus, Rep. Prog. Phys. **67**, 623 (2004).
[4] R. Neutze, R. Wouts, D. van der Spoel, E. Weckert, and J. Hajdu, Nature (London) **406**, 752 (2000).
[5] H. Yoneda *et al.*, Opt. Express **17**, 23 443 (2009).
[6] B. Nagler *et al.*, Nature Phys. **5**, 693 (2009).
[7] L. Young *et al.*, Nature (London) **466**, 56 (2010).
[8] M. G. Makris, P. Lambropoulos, and A. Mihelic, Phys. Rev. Lett. **102**, 033002 (2009).
[9] H. Wabnitz *et al.*, Phys. Rev. Lett. **94**, 023001 (2005).
[10] A. A. Sorokin *et al.*, Phys. Rev. Lett. **99**, 213002 (2007).
[11] A. Rudenko *et al.*, Phys. Rev. Lett. **101**, 073003 (2008).
[12] M. Meyer *et al.*, Phys. Rev. Lett. **104**, 213001 (2010).
[13] N. Berrah *et al.*, J. Mod. Opt. **57**, 1015 (2010).
[14] Y. Hikosaka *et al.*, Phys. Rev. Lett. **105**, 133001 (2010).
[15] M. Nagasono *et al.*, Phys. Rev. A **75**, 051406(R) (2007).
[16] T. Sekikawa, T. Okamoto, E. Haraguchi, M. Yamashita, and T. Nakajima, Opt. Express **16**, 21 922 (2008).
[17] T. Shintake *et al.*, Nature Photon. **2**, 555 (2008).
[18] T. X. Carroll *et al.*, J. Electron Spectrosc. Relat. Phenom. **125**, 127 (2002).
[19] J. Jauhiainen *et al.*, J. Electron Spectrosc. Relat. Phenom. **69**, 181 (1994).
[20] W. Ackermann *et al.*, Nature Photon. **1**, 336 (2007).
[21] P. Emma *et al.*, Nature Photon. **4**, 641 (2010).
[22] W. F. Chan, G. Cooper, X. Guo, G. R. Burton, and C. E. Brion, Phys. Rev. A **46**, 149 (1992).
[23] D. W. Lindle *et al.*, Phys. Rev. A **31**, 714 (1985).
[24] I. Sánchez and F. Martin, Phys. Rev. A **44**, 7318 (1991).
[25] M. Domke, K. Schulz, G. Remmers, G. Kaindl, and D. Wintgen, Phys. Rev. A **53**, 1424 (1996).
[26] L. Lispky, R. Anania, and M. J. Conneely, At. Data Nucl. Data Tables **20**, 127 (1977).
[27] C. D. Lin, Phys. Rev. A **29**, 1019 (1984).
[28] Y. K. Ho, Phys. Rev. A **44**, 4154 (1991).
[29] U. Fano, Rep. Prog. Phys. **46**, 97 (1983).
[30] D. R. Herrick, Adv. Chem. Phys. **52**, 1 (1983).
[31] C. D. Lin, Adv. At. Mol. Phys. **22**, 77 (1986).
[32] C. D. Lin, Phys. Rep. **257**, 1 (1995).
[33] J.-M. Rost, K. Schulz, M. Domke, and G. Kaindl, J. Phys. B **30**, 4663 (1997).
[34] T. Morishita, S. Watanabe, and C. D. Lin, Phys. Rev. Lett. **98**, 083003 (2007).
[35] T. Morishita *et al.*, J. Phys. B **34**, L475 (2001).
[36] R. Moccia and P. Spizzo, Phys. Rev. A **43**, 2199 (1991).
[37] H. A. Bethe and E. E. Salpeter, *Quantum Mechanics of One-and Two-Electron Atoms* (Plenum, New York, 1977).
[38] W. E. Cooke, T. F. Gallagher, S. A. Edelstein, and R. M. Hill, Phys. Rev. Lett. **40**, 178 (1978).
[39] B. Zhou, C. D. Lin, J.-Z. Tang, S. Watanabe, and M. Matsuzawa, J. Phys. B **26**, L337 (1993).
[40] M. Alagia *et al.*, Phys. Rev. Lett. **102**, 153001 (2009).